

Spectrin α II and β II isoforms interact with high affinity at the tetramerization site

Paola A. BIGNONE¹ and Anthony J. BAINES

Department of Biosciences, University of Kent, Canterbury, Kent CT2 7NJ, U.K.

Spectrin tetramers form by the interaction of two α - β dimers through two helices close to the C-terminus of a β subunit and a single helix at the N-terminus of an α subunit. Early work on spectrin from solid tissues (typified by α II and β II polypeptides) indicated that it forms a more stable tetramer than erythroid spectrin (α I- β I). In the present study, we have probed the molecular basis of this phenomenon. We have quantified the interactions of N-terminal regions of two human α polypeptides (α I and α II) with the C-terminal regions of three β isoforms (β I Σ 1, β II Σ 1 and β II Σ 2). α II binds either β II form with a much higher affinity than α I binds β I Σ 1 (K_d values of 5–9 nM and 840 nM respectively at 25 °C). β II Σ 1 and β II Σ 2 are splice variants with different C-terminal extensions outside the tetramerization site: these extensions affect the rate rather than the affinity of α subunit interaction. α II spectrin interacts

with each β subunit with higher affinity than α I, and the β II polypeptides have higher affinities for both α chains than β I Σ 1. The first full repeat of the α subunit has a major role in determining affinity. Enthalpy changes in the α II- β II Σ 2 interaction are large, but the entropy change is comparatively small. The interaction is substantially reduced, but not eliminated, by concentrated salt solutions. The high affinity and slow overall kinetics of association and dissociation of α II- β II spectrin may suit it well to a role in strengthening cell junctions and providing stable anchor points for transmembrane proteins at points specified by cell-adhesion molecules.

Key words: fodrin, spectrin, spectrin dimer self-association, tetramerization of spectrin.

INTRODUCTION

Spectrin is an elongated actin cross-linking protein composed of α and β subunits arranged in a tetramer (reviewed in [1]). α and β subunits align anti-parallel to form a dimer; dimers self-associate head-to-head to form a tetramer. Tetramerization occurs through the interaction of regions close to the N-terminus of α subunits and the C-terminus of β subunits. The physiological requirement for tetramers is exemplified in the haemolytic anaemia hereditary elliptocytosis. Most cases of this condition have their origin in mutations in one or other erythroid spectrin gene, and affect the ability of spectrin to form tetramers [2]. Flies with mutations equivalent to those that cause elliptocytosis in humans are sterile because the egg chambers lose their integrity [3].

The mechanism of erythroid spectrin-tetramer formation has been analysed in great detail [1]. Most of the length of spectrin subunits is made up of triple helices that are imperfect repeats of approx. 106 amino acids (21 or 22 full repeats in α subunits; 16 in 'conventional' β subunits; 30 in β heavy spectrins) (see [4] for a review of spectrin repeats). In both α and β subunits, there are extra partial repeats, and it is these that form the tetramerization site. Two helices in the C-terminal region of β subunits (the partial repeat R17) [In the present report, α or β gene products are designated by roman numerals (α I, α II, β I, β II), and their subtypes generated by splice variation by Σ (thus β II Σ 2 etc.). Triple-helical repeating units within polypeptides are indicated by R and are numbered according to their SwissProt annotations from the N-terminus using arabic numerals (thus β IIIR16 is the 16th repeat of β II spectrin).] can bind to one helix at the N-

terminus of α subunits (partial repeat R1), thereby forming a complete triple helix [5–10]. High-affinity binding also requires the adjacent full triple-helical repeats (α R2 and β R16), and there may be a contribution to the precise binding characteristics of regions in β subunits distal to the triple-helical regions [9,11]. Binding is associated with a conformational change: the total helicity of a mixture of α and β subunits increases as they bind [10,12].

The erythroid spectrin dimer \rightarrow tetramer interconversion has an unusually high activation energy, and moderate affinity (K_d of the dimer-dimer interaction is approx. 3 μ M at 37 °C): the high local concentration of dimers on the cytoplasmic face of erythrocyte cell membranes means that tetramers dominate [13]. Recombinant spectrin fragments containing α I R1–R2 and β I R16–R17 interact with higher affinity than native spectrin (K_d approx. 0.8 μ M) [11]: an energy penalty in native dimers for opening the *cis*-interaction of α and β subunits probably accounts for the difference. Erythroid spectrin is capable of forming higher oligomers (hexamers etc.), but this seems to be much less the case with tissue spectrins, which have a stiffer appearance using electron microscopy [14–17].

Spectrins in mammals are encoded by multiple genes (two α , four conventional β and one β heavy) [1]. It seems that any combination of α and β chains can form dimers. One of the key early observations on spectrin extracted from solid tissues was that it retained its tetrameric state even after warming to 37 °C, although concentrated salt solutions cause partial dissociation to dimers as determined by electron microscopy [15,18]. The gene products that have given rise to stable tetramers have not

Abbreviations used: EDC, *N*-ethyl-*N*'[(3-dimethylamino)propyl]carbodi-imide hydrochloride; GST, glutathione S-transferase; NHS, *N*-hydroxysuccinimide; PH, pleckstrin homology; RU, resonance unit(s); SPR, surface plasmon resonance.

¹ To whom correspondence should be addressed at the present address: Molecular Oncology Laboratory, Cancer Research UK, Weatherall Institute of Molecular Medicine, University of Oxford, John Radcliffe Hospital, Headington, Oxford OX3 9DS, U.K. (e-mail paola.bignone@cancer.org.uk).

been rigorously analysed, but it seems likely that at least α II and β II (fodrin) are associated with stable tetramers, since these are abundant and ubiquitous in solid tissues.

A common characteristic in the β spectrins is C-terminal splice variation. We have defined a splice variation in β II spectrin that gives rise to 'long' or 'short' C-terminal variants [19]. The long form (β II Σ 1) has a pleckstrin homology (PH) domain separated from the triple-helical repeats by a flexible linker region. A splicing event midway through exons encoding the linker changes the C-terminal region so that a short form (β II Σ 2) lacks the PH domain, and has instead a unique short region devoid of any known structural domain(s).

The molecular mechanism(s) that define the relative stability of tissue spectrin tetramers have not previously been the subject of investigation. In the present study, we have probed this using recombinant polypeptides analogous with those used to define erythroid spectrin subunit interactions. We find that α II spectrin is associated with much higher-affinity interactions than α I, and that the β II spectrins interact with α II with very high affinity. We have analysed the interaction of α II and β II Σ 2 in detail to give a view of the fundamental nature of the tissue spectrin α - β interaction. These results are discussed in the context of genetic definition of spectrin as a molecule required for stabilization of intercellular junctions.

EXPERIMENTAL

Materials

cDNAs encoding α I spectrin N-terminus-R2 and β I Σ 1 R16-C-terminus (amino acids 1898–2137) were kindly provided in the vectors pGEX-2T and pGEX-KG respectively [11] by Dr Marie-Christine Lecomte (INSERM, Paris, France). Total human skeletal muscle cDNA (Multiple Choice, Origene) was purchased from Cambridge Biosciences (Cambridge, U.K.).

The BIAcore 2000 system, CM5 chips, surfactant P20, *N*-hydroxysuccinimide (NHS), *N*-ethyl-*N'*[(3-dimethylamino)propyl]-carbodi-imide hydrochloride (EDC), 1 M ethanolamine/HCl, pH 8.2, 10 mM sodium acetate, pH 5.0, 10 mM glycine, pH 2.0, 10 mM glycine, pH 3.0, and normalizing solution were from BIAcore AB (Stevenage, Herts., U.K.). Monoclonal anti-(glutathione S-transferase) (GST) antibody (mouse ascites fluid) was from Sigma (catalogue number G1160).

Recombinant polypeptides

GST- α I human spectrin was expressed and isolated as described by Nicolas et al. [11].

GST- α II was obtained as follows. Nested PCR was performed using *Pfu* polymerase (Promega), human skeletal muscle cDNA and primer pairs F-nested- α II/R-nested- α II, R-GST- α II/F-GST- α II (see Table 1). The 446 bp PCR product encoded residues 1–145 of human α II spectrin. It was digested with *Bam*HI and *Eco*RI, and ligated into pGEX-2T (Amersham Biosciences) for expression of GST- α IIR1-R2.

Chimaeras of α I and α II were produced in which R1 was from one α subunit, and R2 was from the other. A unique *Bsr*BRI restriction site exists at the 3' end of the cDNA encoding R1 in both α I and α II. cDNA encoding either α I or α II was digested with *Bsr*BRI and *Eco*RI; the resulting fragments were used to generate chimaeras α I- α II (containing α I R1 fused to α II R2) or α II- α I (containing α II R1 fused to α I R2). These chimaeras were expressed as GST-fusion proteins, as described for the other α constructs.

Table 1 Primers used for generating constructs used in this study

Oligonucleotides designed for the directional cloning of spectrin fragments in pRSET-a and pGEX-2T vectors using the restriction sites are shown in bold in the sequence. The target is specified by its GenBank® accession number and the residues where the primer anneals. See text for more details.

Primer name	Sequence	Target
F-nested- α II	5'-GCGGAGGCTCCTCGGTCTTCA-3'	M61877 31–52
R-nested α II	5'-TGCCAGGTCTCGGCCAAAATCA-3'	M61877 945–966
R-GST- α II	5'- GGAATTC TGACAATTTGATTCCTTTTCTCG-3'	M61877 517–537
F-GST- α II	5'-GAGGATCCAAAATGGACCCAAGT-3'	M61877 100–114
F-His- β II	5'-CTC CTCGAG GCCTGTGAGAGC-3'	M96803 5996–6016
R-His- β II Σ 1	5'-GGT AAGCTT AGGGCAGGAGGTG-3'	M96803 7418–7430
R-His- β II Σ 2	5'-GGGT AAGCTT GACAAATGGTAG-3'	AJ005694 256–270

To generate His-tagged β spectrin constructs, cDNAs were cloned into the vector pRSETa (Invitrogen). Human β I Σ 1 was subcloned directly from the vector in which it was supplied using *Hind*III and *Bam*HI. Spectrin β II Σ 1 and β II Σ 2 cDNAs were obtained by amplification of human skeletal muscle cDNA using primer pairs (β II Σ 1) F-His- β II/R-His- β II Σ 1 or (β II Σ 2) F-His- β II/R-His- β II Σ 2. Each construct was verified by nucleic acid sequencing (using the services of MWG-Biotech, Milton Keynes, U.K.).

Recombinant polypeptides were expressed in *Escherichia coli* BL21 (DE3) or C41 (DE3). Expression was induced using isopropyl β -D-thiogalactoside (IPTG), and bacteria were lysed by sonication. Recombinant proteins were purified from the soluble portions of lysates by affinity chromatography on glutathione-Sepharose (for GST-fusions) or chelating columns [HisTrap (Amersham Biosciences) for His-tagged proteins].

Purified constructs were assessed for correct folding in two ways. They were analysed by CD spectrometry in a Jasco J-600 spectropolarimeter using quartz cuvettes with path length of 0.05 cm at 18.5 °C. Protein concentration was assessed at A_{280} using the molar absorption coefficient calculated based on the tryptophan, tyrosine and cystine residues in the recombinant protein [20]. The CD data presented represent the mean of eight runs between wavelengths of 195 nm and 250 nm, less the contribution of the buffer (20 mM sodium phosphate, pH 7.4, and 150 mM NaCl), and converted into mean residue molar ellipticity, expressed in degrees \cdot cm⁻² \cdot dmol⁻¹ as in [12]. Recombinant proteins were also subjected to limited proteolysis [21] using chymotrypsin. Briefly, recombinant proteins were digested at 0 °C in 0.1 M Tris/HCl, pH 8.0, with chymotrypsin [enzyme/substrate ratio of 1:100 or 1:500 (w/v)] for 20–180 min. Digestion products were analysed by SDS/PAGE and Western blotting [22]. Potential self-association of the constructs was assessed by gel filtration on a Superose 12HR column (1 cm \times 30 cm; Amersham Biosciences), as described in [22].

Pull-down assays for binding

GST- α II (0–1.12 μ M) and His-tagged β II Σ 2 polypeptides (0.75 μ M) were incubated for at least 3 h at 22 °C in 10 mM Hepes, pH 7.4, 150 mM NaCl, 3 mM EDTA and 0.005 % (v/v) Tween 20. The reaction mixture (50 μ l) was transferred on to a MicroSpin column (Amersham Biosciences), containing 20 μ l of a 75 % slurry of glutathione-Sepharose 4B equilibrated in binding buffer, and incubated for 30 min. Unbound proteins were recovered by centrifugation at 750 g for 1 min. The Sepharose was washed three times with 500 μ l of 10 mM Hepes, pH 7.4,

150 mM NaCl, 3 mM EDTA and 0.2% (v/v) Tween 20. Bound proteins were eluted with 40 μ l of 1 \times Laemmli sample buffer [23]. Samples were boiled for 5 min and loaded on a 12% (w/v) polyacrylamide/SDS gel [23]. In control reactions, GST alone was used, and blanks with no GST proteins were also run. Samples were analysed by immunoblotting and probing with anti-His₅ antibody (Qiagen) for the presence of His-tagged β subunits. Immunoblots were developed with ECL[®] (Amersham Biosciences) reagents, and, for densitometric analysis, several timed exposures were made from each film to ensure the linearity of response.

BIAcore surface plasmon resonance (SPR) assays

Binding reactions were done in HBS-EP buffer, containing 20 mM Hepes, 150 mM NaCl, 3 mM EDTA and 0.005% (v/v) surfactant P20, pH 7.4, filtered (0.4 μ m) and degassed before use. Recombinant proteins were dialysed against HBS-EP buffer; solutions were centrifuged at 15000 g for 30 min at 4 °C or passed through a 0.2 μ m filter to remove any aggregated material formed during dialysis.

Amine-coupling of proteins to the sensor surface

An anti-GST surface was created on CM5 sensor chips by immobilization of monoclonal anti-GST antibody. The carboxymethyl-dextran surface of the chip was activated with a 70 μ l injection of a mixture of 0.1 M NHS and 0.1 M EDC in water. To couple the antibody, an aliquot of 50 μ l of a 1/250 dilution of the antibody in 10 mM sodium acetate, pH 5.0, was used, obtaining levels of 5000–6000 resonance units (RU) for the immobilization. The remaining NHS-ester active sites in the dextran were blocked with 70 μ l of 1 M ethanolamine, pH 8.2, and washed at a higher flow rate, 20 μ l \cdot min⁻¹, with two pulses of 10 μ l of 10 mM glycine, pH 2.5.

Capture of ligand

Purified GST-fusion proteins or GST were captured on to the anti-GST surface by injecting an aliquot of a 0.1 μ M or 1 μ M solution of the protein, in HBS-EP buffer, at 5 μ l \cdot min⁻¹. To remove any loosely bound protein, a regeneration cycle was performed before assessing this surface for binding.

Regeneration conditions

The regeneration conditions developed in the present study involved a high-salt wash [20 mM Hepes, pH 7.4, 2 M KCl, 3 mM EDTA and 0.005% (v/v) surfactant P20], followed by mild urea wash (3 M urea, 20 mM Hepes, pH 7.4, 0.1 M glycine and 2 M KCl). For the regeneration of the GST surfaces, cycles of high-salt buffer and urea buffer with contact times of 240 s were used; if the absolute response of the flowcell was more than 20 RU higher than the baseline level at the beginning of the experiment, a second cycle was applied to the surface. This regeneration was followed by a stabilization step of buffer flowing over the chip for 5 min.

Kinetic analysis of binding

For kinetic characterization of the interaction, GST-fusion proteins were captured on an anti-GST surface at low levels, 75–150 RU. GST was captured in a reference cell at equimolar level.

In order to minimize mass transport effects, binding analyses were performed at flow rates of 20 μ l \cdot min⁻¹ at 25 °C or at the temperature specified in the text. Analyte (100 μ l) was injected into the instrument, and the association of analyte and ligand was recorded. After this, the surface was washed with buffer for 360 s to follow the dissociation of analyte–ligand complexes. To maximize reproducibility between analyses, the BIAcore instrument was programmed to perform a series of experiments with increasing concentrations of analyte over the same regenerated surface.

Equilibrium titration

Buffer was injected over GST-fusion protein surfaces to determine the baseline, then solutions of increasing concentration of analyte (180 μ l at 5 μ l \cdot min⁻¹ at 25 °C) were injected when the interaction for a previous concentration reached close to a plateau.

Data analysis

Thermodynamic analyses followed the guidelines given by Myszkla [24] and Zeder-Lutz et al. [25]. Sensorgrams (plots of changes in RU on the surface as a function of time) of the interaction generated by the instrument were analysed using the software BIAeval 3.0 (BIAcore AB). The quality of the data was improved by double referencing [24]. Signal at the beginning of the sensorgram was zeroed using the mean of the response 20 s before the injection. The reference surface data were subtracted from the reaction surface data to eliminate refractive-index changes of the solution, injection noise and non-specific binding to the GST moiety and the modified surface. Finally, a blank injection with buffer was subtracted from the resulting reaction surface data. Sensorgrams for each concentration analysed were processed individually and were then overlaid. Data were globally fitted to the Langmuir model for an homogeneous, univalent and reversible interaction. When there were discrepancies between the data and the model, the bivalent model of the interaction was tested. In both cases, the model data were fitted to the experimental data using the non-linear least-squares fitting processes, available in BIAeval software.

For analysis of equilibrium-titration data, a mean of response values was taken from 1700 s to 2150 s after the start of each injection; these corresponded to the amount of complex formed at each analyte concentration. Responses were plotted against the analyte concentration to obtain binding curves for the interaction.

RESULTS

Recombinant spectrin polypeptides

To assay the interactions of α and β spectrin polypeptides, we required recombinant proteins that would accurately recapitulate the interactions of the native proteins. We designed constructs that included the partial triple-helical segments that contain the binding sites, plus the neighbouring full repeats. These were fused to GST (α) or a His tag (β). Figures 1(a) and 1(b) show the constructs schematically, and Figure 1(c) shows Coomassie-Blue-stained gels of each.

To verify that the proteins accurately represented the native state, they were analysed for folding and self-association state. The proteins contained chymotrypsin-resistant units that corresponded to the repeats [21]. In the case of the α constructs and the chimaeric proteins, repeat 2 was cleaved by chymotrypsin as

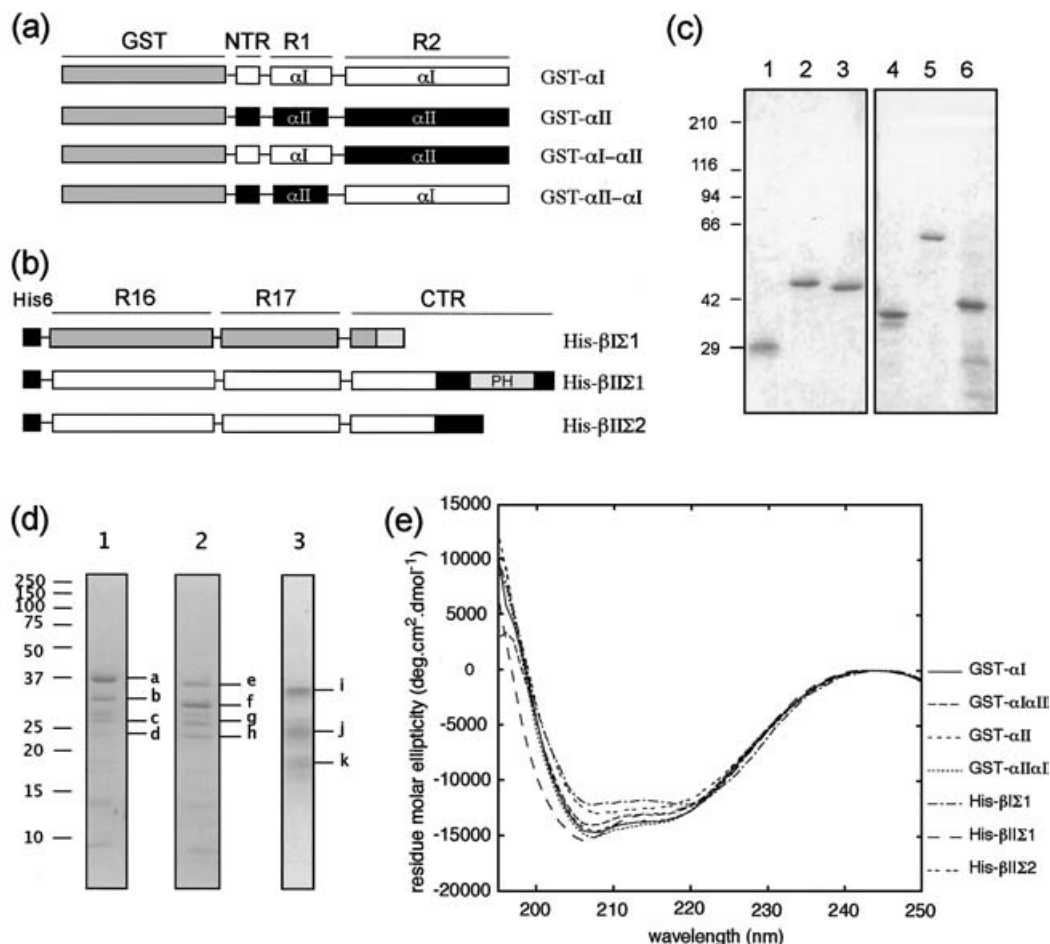


Figure 1 Constructs used in the present study

GST- and His-tagged constructs were prepared as described in the text. **(a)** Schematic representation of α -spectrin constructs. NTR, N-terminal region; R1, partial triple-helical repeat that binds to β subunits; R2, first full triple helix. α I- α II and α II- α I are chimaeras in which R1 and R2 are swapped between the proteins. **(b)** β -Spectrin constructs. R16, last full triple helix in β ; R17, partial repeat containing helices A and B of the triple helix: this interacts with helix C provided by α R1; CTR, C-terminal regions that are unique to each protein; PH, pleckstrin homology domain in β II Σ 1, the long C-terminal variant. **(c)** Constructs analysed by SDS/PAGE. Lane 1, GST alone; lane 2, GST- α I; lane 3, GST- α II; lane 4, His- β I Σ 1; lane 5, His- β II Σ 1; lane 6, His- β II Σ 2. **(d)** Limited chymotrypsin digestion of representative constructs, at 1:100 ratio for 30 min, electrophoretically separated by SDS/10–20% gradient PAGE, stained with Coomassie Blue (CB). Chymotryptic fragments for GST- α I (lane 1) are: a, GST- α INTR- α IR1- α IR2 (undigested GST- α I); b, GST- α INTR- α IR1; c, GST- α INTR; d, GST. Chymotryptic fragments for GST- α II α I (lane 2) are: e, GST- α INTR- α IR1- α IR2 (undigested GST- α II α I); f, GST- α INTR- α IR1; g, GST- α INTR; h, GST. Chymotryptic fragments for His- β II Σ 2 (lane 3) are: i, His- β IR16- β IR17- β II Σ 2CTR (undigested His- β II Σ 2); j, His- β IR16- β IR17; k, His- β IR16. **(e)** Far-UV spectra of purified GST-fusion proteins expressing the N-terminal of the α subunits of spectrin and the chimaeric proteins and His-tagged proteins expressing the C-terminal of β spectrin, obtained at 18.5 °C, in 20 mM sodium phosphate, pH 7.4, and 150 mM NaCl.

a unit, and afterwards, the incomplete repeat 1 and N-terminal, leaving the GST moiety (Figure 1d, lanes 1 and 2). In the case of the β constructs, the most labile parts were the C-terminal extensions. Repeats 16 and 17 remained together in a single fragment after all the C-terminal regions had been removed, indicating their relative stability (Figure 1d, lane 3). Extended digestion [180 min, enzyme/substrate ratio 1:100 (w/v)] left repeat 16 as the sole remaining intact structure. The full triple helix of repeat 16 is, as expected, very stable to chymotrypsin. CD revealed a similar conformation in terms of α -helix content in all the constructs (Figure 1e) (see [12]); this gives confidence that the structure of the α I- α II and α II- α I chimaeras are similar to the α I and α II prototypes. The β constructs were more variable in their CD spectra, which reflects the variable nature of their C-termini: β II Σ 1 has a PH domain absent from the others; β I Σ 1 and β II Σ 2 have C-terminal extensions of unknown structure. The constructs were found to be monomeric by gel filtration: in fresh preparations, no dimer or higher species of aggregate was

found. We conclude that the constructs were correctly folded and monomeric.

Pull-down assays indicate a high-affinity interaction between α II and β II Σ 2

As a preliminary to detailed analysis, the interaction between α II and β II Σ 2 constructs was measured in a simple pull-down assay. In this, a fixed concentration of β II Σ 2 was mixed at 25 °C with various concentrations of α II as described in the Experimental section. At end of the reaction, glutathione beads were added to capture α II construct. The beads were washed and bound proteins recovered; the relative amounts of both constructs bound were determined by gel electrophoresis and immunoblotting. Figure 2 shows the result of such an experiment. The data fitted well to a single class of binding site, with a K_d of 28.8 ± 3.3 nM. This indicates a much higher-affinity interaction than is known between α I and β I. In control reactions, GST alone was mixed with the

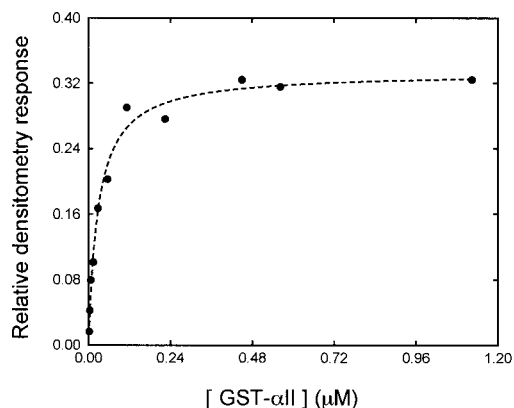


Figure 2 Pull-down assay for α II- β II Σ 2 interaction

β II Σ 2 (0.75 μ M) was incubated for 3 h at 22 $^{\circ}$ C either alone or in the presence of differing amounts of GST- α II (ranging from 0 to 1.12 μ M) in a final reaction volume of 50 μ l. Free and bound species were separated with glutathione-Sepharose beads. Complexed His-tagged proteins were quantified from Coomassie-Blue-stained gels or from immunoblots with anti-His antibodies by densitometry. The α II/ β II Σ 2 molar ratio in complexes where α II was limiting approximated to 1:1. The line shown is calculated for K_d of approx. 28.8 ± 3.3 nM.

β II Σ 2, and no binding was detected. Therefore, GST itself did not comprise a binding site in GST- α II.

SPR assay for interactions

To analyse the interaction of various α and β constructs in more detail, a SPR assay was developed (Figure 3a). In this assay, antibody against GST was coupled to the surface of a BIAcore CM5 chip, as described in the Experimental section. On this, GST- α was captured. This provides a stable surface, with a rate of GST- α loss of approx. 0.03 RU/s. This method of capture has other advantages: the antibody does not modify the α moiety, which is oriented away from the capture surface. In the four channels of a BIAcore 2000 instrument, it was possible to capture, in parallel, two GST- α constructs and GST alone; the remaining lane where no GST was captured was a blank channel. To ensure that the binding to be measured was not limited by mass transport effects, the total level of captured GST- α was kept to the minimum practical level: 120–150 RU was captured for GST- α , with equivalent molar amounts for GST alone in control channels.

β Polypeptides were run through each channel, and binding was followed as an increase in signal from the surface. For kinetic

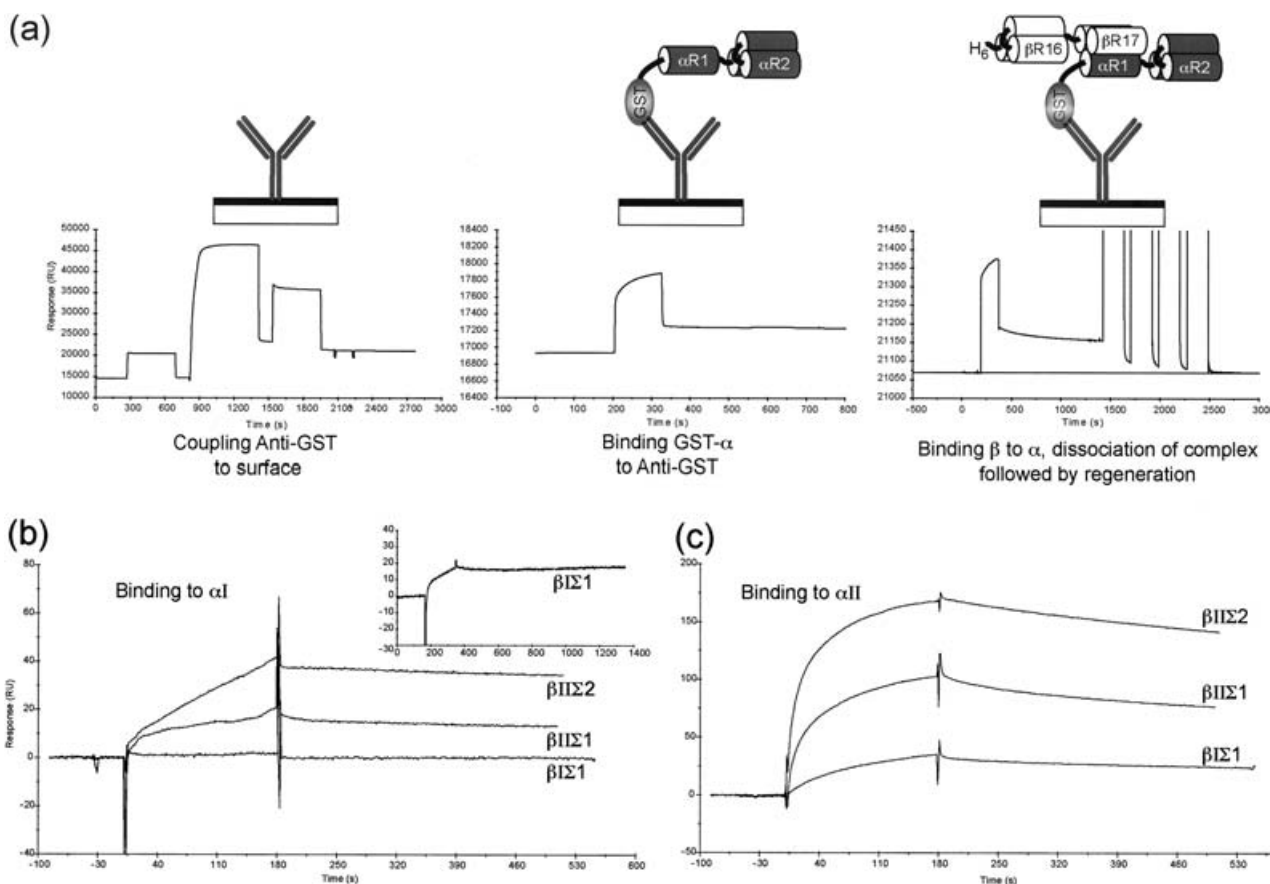


Figure 3 SPR assay for α - β spectrin interaction

(a) Experimental design for the study of spectrin interactions using BIAcore. An anti-GST antibody surface was created on CM5 sensor chips using amine coupling (left-hand panel). Recombinant GST- α or GST was captured on to the anti-GST surface in different flowcells (centre panel). β -Spectrin solutions were injected, and binding was followed as an increase in the response during the association phase and a decrease in the response during the dissociation of the complex; in the raw data, an important component of the signal was the bulk refractive index of the solution. Bound proteins were washed away during regeneration cycles, corresponding to the last portion of this sensorgram (right-hand panel). (b) and (c) Sensorgrams for the interaction of recombinant C-termini of β -spectrin with N-termini of α -subunits. (b) GST- α I and (c) GST- α II were captured on to an anti-GST surface at 150–170 RU. Specific binding of each recombinant protein was obtained by subtracting a reference sensorgram corresponding to captured GST at equimolar levels. Interactions are shown for 1 μ M solutions of His-tagged proteins at 20 μ l \cdot min $^{-1}$. The inset in (b) shows the binding of β I Σ 1 to a surface of α I containing 400 RU of immobilized protein.

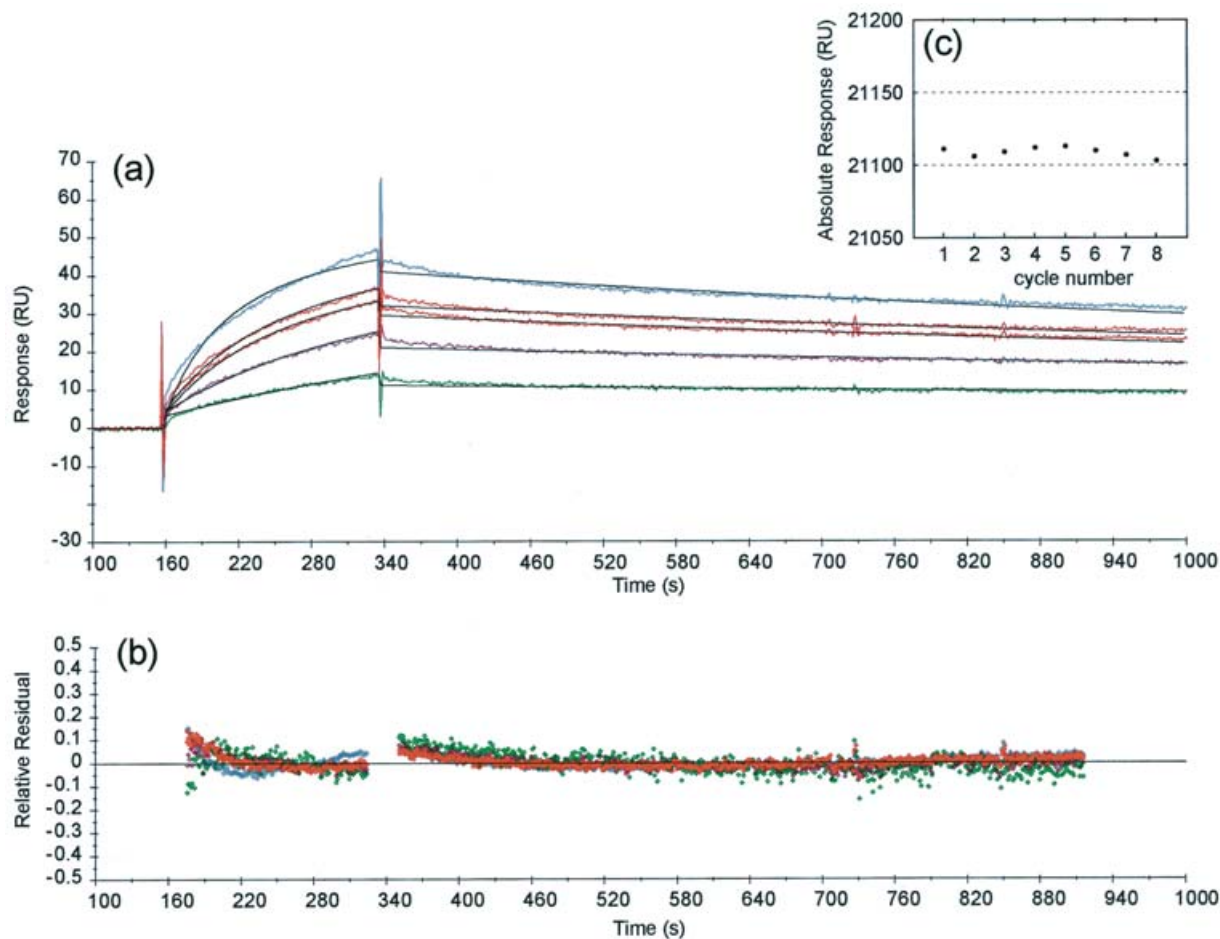


Figure 4 Kinetic analysis of α II- β II Σ 2 interaction

β II Σ 2 at different concentrations (0.2, 0.5, 1.0, 1.5 and 2.0 μ M from bottom to top) was injected at 20 μ l \cdot min $^{-1}$ over 150 RU of GST- α II in a BIAcore 2000 instrument. Double-referenced sensorgrams were globally fitted to a bivalent reversible-interaction model; black lines over the experimental data (a) showed the non-linear regression analysis, and the relative residual for each curve was calculated (b). (c) To test the robustness of the surface, the binding reaction was repeated eight times at a single concentration of β II Σ 2, and the absolute response at the beginning of each cycle is shown. Note that there is no detectable loss of GST- α II, or build-up of bound protein.

analyses, the signal from the GST alone and blank channels were subtracted from the channel containing the α construct of interest as described in the Experimental section. In this way, any signal deriving from GST was subtracted from the α subunit, and any changes in signal due to refractive-index changes were eliminated.

To regenerate the surface for repeated rounds of binding, a regeneration method based on the known properties of erythroid spectrin was developed. Urea (3 M) separates erythroid spectrin into its component subunits; removal of urea allows re-formation of spectrin dimers and tetramers [26]. We applied this knowledge to regeneration of the surface between rounds of binding. To strip bound β subunits from the surface, washes of 3 M urea and 2 M KCl were passed through the channels as described in the Experimental section. This removed all β subunits, without affecting the level of α subunits remaining, or its ability to bind β chains after washing back into urea-free buffer solution.

Figures 3(b) and 3(c) show the interactions of α I and α II respectively with the various β constructs. Note the considerable variation in observed association rates, and, in particular, that with the low concentration of α I used, interaction with β I Σ 1 (erythroid β -spectrin) was below the detection limit. However, the α I- β I Σ 1 association was detected when higher quantities of α I were immobilized on a BIAcore chip (Figure 3b, inset).

As described below, the measured association properties are as expected for this polypeptide, and the apparent lack of binding observed in Figure 3(b) merely reflects the conditions used and the comparative strength of the other interactions.

Kinetic analysis of interactions

To quantify the interactions of α and β polypeptides in the SPR assay, binding of all permutations of α constructs (α I, α II plus the chimaeras α I- α II and α II- α I) and β constructs (β I Σ 1, β II Σ 1 and β II Σ 2) were analysed. Figure 4(a) shows an example of the time course of α II binding to five concentrations of β II Σ 2. In the first part of the Figure, β II Σ 2 is seen associating with α II. After 340 s of association, buffer was run over the surface to allow dissociation of bound complexes. The signal decreased slowly over time. The data were analysed by GlobalFit in the BIAeval program. Calculated curves fitted to the data (shown in black) are superimposed on the observed data (shown in colour). Figure 4(b) indicates the data fits well to each curve: residuals (the difference between observed and calculated data points) are very small (note the scale).

To ensure reproducibility of the assay, a single concentration of β II Σ 2 was repeatedly run over the surface (Figure 4c). When eight

Table 2 Affinity and kinetic constants for the interaction of recombinant C-termini of β -spectrin with N-termini of α -subunits

Rate constants for the association (k_{on} , $\text{M}^{-1} \cdot \text{s}^{-1}$) and dissociation (k_{off} , s^{-1}) were calculated for each pair of recombinant proteins using kinetic measurements of the interactions. Rate constants $k_{1,\text{on}}$ and $k_{1,\text{off}}$ referred to the high-affinity site calculated when the interaction was best fitted to the bivalent interaction model. The equilibrium dissociation constant (K_d) was calculated as $k_{\text{off}}/k_{\text{on}}$ or $k_{1,\text{off}}/k_{1,\text{on}}$. The S.E.M. shown for K_d was estimated from the errors associated with k_{on} and k_{off} , or $k_{1,\text{on}}$ and $k_{1,\text{off}}$.

	α I			α II			α I- α II			α II- α I		
	k_{on}	k_{off}	K_d	$k_{1,\text{on}}$	$k_{1,\text{off}}$	K_d	k_{on}	k_{off}	K_d	$k_{1,\text{on}}$	$k_{1,\text{off}}$	K_d
β I Σ 1	59.4	5×10^{-5}	841.8 ± 79.6	2900	8×10^{-4}	275.9 ± 4.1	3020	1.3×10^{-3}	430.5 ± 3.4	1470	1.1×10^{-3}	748.3 ± 17.3
β II Σ 1	4450	3×10^{-4}	67.4 ± 2.1	266220	1.2×10^{-3}	4.5 ± 2.2	13600	5×10^{-4}	36.8 ± 0.8	15600	6.2×10^{-4}	38.5 ± 3.0
β II Σ 2	14800	9×10^{-4}	60 ± 7.5	24700	2.1×10^{-4}	8.5 ± 2.0	4200	3×10^{-4}	71.4 ± 0.9	6680	4×10^{-4}	59.9 ± 2.8

cycles of binding and regeneration were performed on the same GST surface, the change in baseline at the beginning of each cycle was between +3 and -8 RU. The binding of the GST moiety to the anti-GST antibody surface was not disturbed by the regeneration buffers, since no losses of GST were detected in the flowcell control. After eight cycles of binding and regeneration, 98% of the binding level observed in the first cycle was retained.

Table 2 summarizes the data obtained from kinetic analysis of the interactions. Note that α II binds with higher affinity to all constructs than α I. β II polypeptides generally bind with higher affinity to either α subunit than β I Σ 1. α II- β II interactions are the strongest; the measured K_d (5 nM for α II- β II Σ 1; 9 nM for α II- β II Σ 2) by equilibrium titration and by pull-down assay (Figure 2) is < 30 nM, different from the 900 nM reported for erythroid spectrin [11], giving added confidence in a high-affinity interaction for α II- β II. The variable C-terminal extension makes no substantial difference to the affinity, although the rate constants vary between the long C-terminal variant (β II Σ 1) and the short (β II Σ 2). Clearly, the C-terminal extensions have an effect on both the rate of association (compare, for example, α II- β II Σ 1 k_{on} , $266220 \text{ M}^{-1} \cdot \text{s}^{-1}$, with α II- β II Σ 2 k_{on} , $24700 \text{ M}^{-1} \cdot \text{s}^{-1}$) and dissociation (k_{off} , $1.2 \times 10^{-3} \text{ s}^{-1}$ and $2.1 \times 10^{-4} \text{ s}^{-1}$ respectively), but the effects of these on the affinity are comparatively small (the affinities are considered similar for an interval of confidence of $K_d \pm 2$).

α I- β I Σ 1 is the weakest interaction, but the measured K_d is very similar to that obtained by others (842 nM, see Table 2; 900 nM by Nicolas et al. [11], also see comments in the Discussion section). Note also the extremely low dissociation rate constant for this interaction.

The chimaeras reveal that the binding characteristics of each construct are not dictated by only the partial triple helices (α R1 and β R17), but that other interactions also participate. The α II- α I chimaera binds β I Σ 1 with an affinity ($K_d = 748 \text{ nM}$) similar to α I ($K_d = 842 \text{ nM}$). The α I- α II chimaera binds with somewhat higher affinity ($K_d = 431 \text{ nM}$), although not as strongly as α II binds ($K_d = 276 \text{ nM}$). β II Σ 1 binds both chimaeras with affinities (K_d for α I- α II = 37 nM; K_d for α II- α I = 39 nM) intermediate between the interactions with native α I (67 nM) or α II (5 nM). These data indicate joint roles for α R1 and α R2 in determining affinity. Most importantly, R2 of α subunits evidently has a role in dictating the characteristics of interaction with β subunits that has not been documented previously.

Interestingly, β II Σ 2 binds α II- α I ($K_d = 60 \text{ nM}$) indistinguishably from α I ($K_d = 60 \text{ nM}$), and similar to α I- α II ($K_d = 71 \text{ nM}$), but different from α II ($K_d = 9 \text{ nM}$). Since the two β II isoforms do not behave identically, this argues for additional interactions, in which the C-terminal extensions of the β splice variants play a part in determining affinities, even if this is not manifest in the native α I and α II interactions.

Equilibrium titration

To provide a further view of the interaction, equilibrium titration was used. In this, the SPR association phase is followed until a plateau is reached; the concentration of analyte is then increased, and association is followed to a new plateau. With successive increases, the plateau level can be determined and used to estimate a K_d . Figure 5 shows an equilibrium titration experiment for α II- β II Σ 2. Figure 5 (inset) shows the data plotted in the form of a Scatchard plot. The line shown is calculated for a K_d of approx. $9.5 \pm 0.5 \text{ nM}$, in good agreement with all the analyses described above.

Thermodynamic analysis of interactions

The BIAcore can be operated at different temperatures, giving the opportunity for thermodynamic analysis of the interactions. Figure 6(a) shows temperature-dependence of the α II- β II Σ 2 interaction. For simplicity, Figure 6(a) only shows curves for four temperatures, but measurements were made for six different temperatures (five analyte concentrations per temperature point), as indicated in Figures 6(b) and 6(c), and in Table 3. We were unable to obtain good measurements at 37 °C, because the constructs were somewhat unstable at this temperature.

The rates of both association and dissociation increase as the temperature is raised. Overall, increasing temperature reduces the affinity.

The free-energy change is related to the equilibrium constant by eqn 1:

$$\Delta G^\circ = -RT \ln K_d \quad (1)$$

ΔG° is the Gibbs free energy change at the reference temperature (25 °C), R is the gas constant ($8.314 \text{ J} \cdot \text{mol}^{-1} \cdot \text{K}^{-1}$), T is the absolute temperature (K) and K_d is the dissociation constant. For the reference state, it was calculated as $\Delta G^\circ = -45.5 \text{ kJ} \cdot \text{mol}^{-1}$ (from a K_d of 9.5 nM).

Using the van't Hoff relationship (eqn 2), the dissociation constants for the interaction throughout the temperature range studied were correlated with the enthalpy change for the interaction.

$$\ln K_d = \frac{\Delta H^\circ}{RT} + \frac{\Delta S^\circ}{R} \quad (2)$$

The values of the enthalpy change, and the entropy change for the interaction between α II and β II Σ 2, calculated from the linear regression of the experimental data (Figure 6b), are summarized in Table 4(a). The enthalpy change was substantial, $-245 \text{ kJ} \cdot \text{mol}^{-1}$. These data suggest that enthalpy change plays a major part in α II- β II Σ 2 interaction.

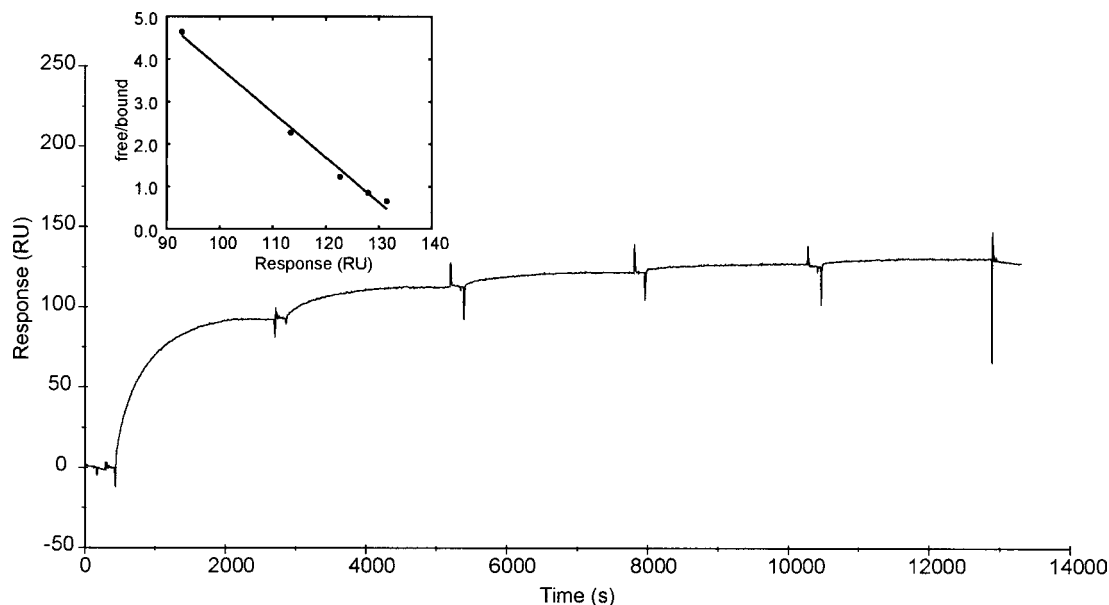


Figure 5 Equilibrium titration of α II- β II Σ 2

Sensorgram of immobilized GST- α II sequentially equilibrated with solutions of β II Σ 2 at concentrations ranging from 0.2 to 2 μ M, at a flow rate of 5 μ l \cdot min $^{-1}$. Responses at the equilibrium (1700–2150 s of each injection) were plotted against the β II Σ 2 starting solution concentration. The data were plotted in the form of a Scatchard plot (inset). The line shown is calculated for K_d of approx. 9.5 \pm 0.5 nM.

Eqn 3 defines a Gibbs free energy change associated with the transition state:

$$\Delta G^\ddagger = -RT \ln(kh/k_B T) \quad (3)$$

In this equation, ΔG^\ddagger is the Gibbs free-energy change for the transition state, k is a rate constant for the reaction, h is Planck's constant (6.626×10^{-34} J \cdot s), k_B is Boltzmann's constant (1.3807×10^{-23} J \cdot K $^{-1}$). Using the value of the dissociation rate constant at the reference temperature, ΔG^\ddagger is 94.0 kJ \cdot mol $^{-1}$.

An Eyring plot of the dissociation rate constants (eqn 4 and Figure 6c) was used to obtain the enthalpy of activation (ΔH^\ddagger). The corresponding contribution of the entropy change for the formation of the transition state was calculated from $\Delta G_d^\ddagger = \Delta H_d^\ddagger - T \cdot \Delta S_d^\ddagger$. Transition state values are summarized in Table 4(b).

$$\ln\left(\frac{kh}{k_B T}\right) = \left(\frac{-\Delta H^\ddagger}{RT}\right) \cdot \left(\frac{1}{T}\right) + \left(\frac{\Delta S^\ddagger}{R}\right) \quad (4)$$

From all the parameters estimated, a free-energy profile of the interaction between the N-terminus of α II and the C-terminus of β II Σ 2 is presented in Figure 6(d).

Ionic-strength dependence of the interaction

The interaction of α II and β II Σ 2 was dependent on the ionic strength of the medium. Binding of 1 μ M β II Σ 2 to α II was measured in solutions similar to HBS-EP, but with the indicated concentration of NaCl.

Different binding levels were observed with the same protein concentration at varying ionic strength (Figure 7). At 0 and 10 mM NaCl, binding levels were negligible. Binding appeared maximal at approx. 100 mM NaCl, indicating that maximum binding occurred in physiological solutions. At higher concentrations of

NaCl (\geq 300 mM), binding levels were reduced, but seemed to stabilize at approx. 30% of maximum.

DISCUSSION

It has been apparent since the non-erythroid spectrins were first purified some 20 years ago that they form more stable tetramers than erythroid spectrin. To investigate the molecular mechanisms underlying this, we have generated recombinant fragments of the abundant non-erythroid α II and β II spectrins (see Figure 1) and quantified their interactions *in vitro*. The β chains have splice variation near the C-terminus, which could potentially affect binding to α subunits, so we included both the 'long' C-terminal variant, β II Σ 1, and the 'short' β II Σ 2 in the analysis. For detailed analysis of the binding, we concentrated on α II and β II Σ 2 spectrin: the short C-terminal β II variant is comparatively easy to work with, and is of great physiological interest, since it is abundant in both brain and heart [19]; α II is the most abundant α chain in solid tissues. It was only possible to work with recombinant fragments of these proteins: no method has yet been established for preparation of recombinant spectrin tetramers from cloned cDNAs.

Both 'pull-down' and SPR assays were developed to measure the interaction. The advantage of using the BIAcore instrument over other techniques to study the interaction of spectrin subunits is that formation of the complex is followed in real-time, without the need to separate free and bound species of the complex. Capturing the GST-fusion protein on to an anti-GST surface meant that the α subunit faced free solution, and was not covalently modified if directly captured on the chip; in all cases, parallel flowcells with equimolar levels of purified GST were run as a control. Binding surfaces were regenerated by removing the bound β subunit; this allowed the re-use of the same surface for further experiments, keeping conditions very similar throughout a series of measurements. Good regeneration was obtained without

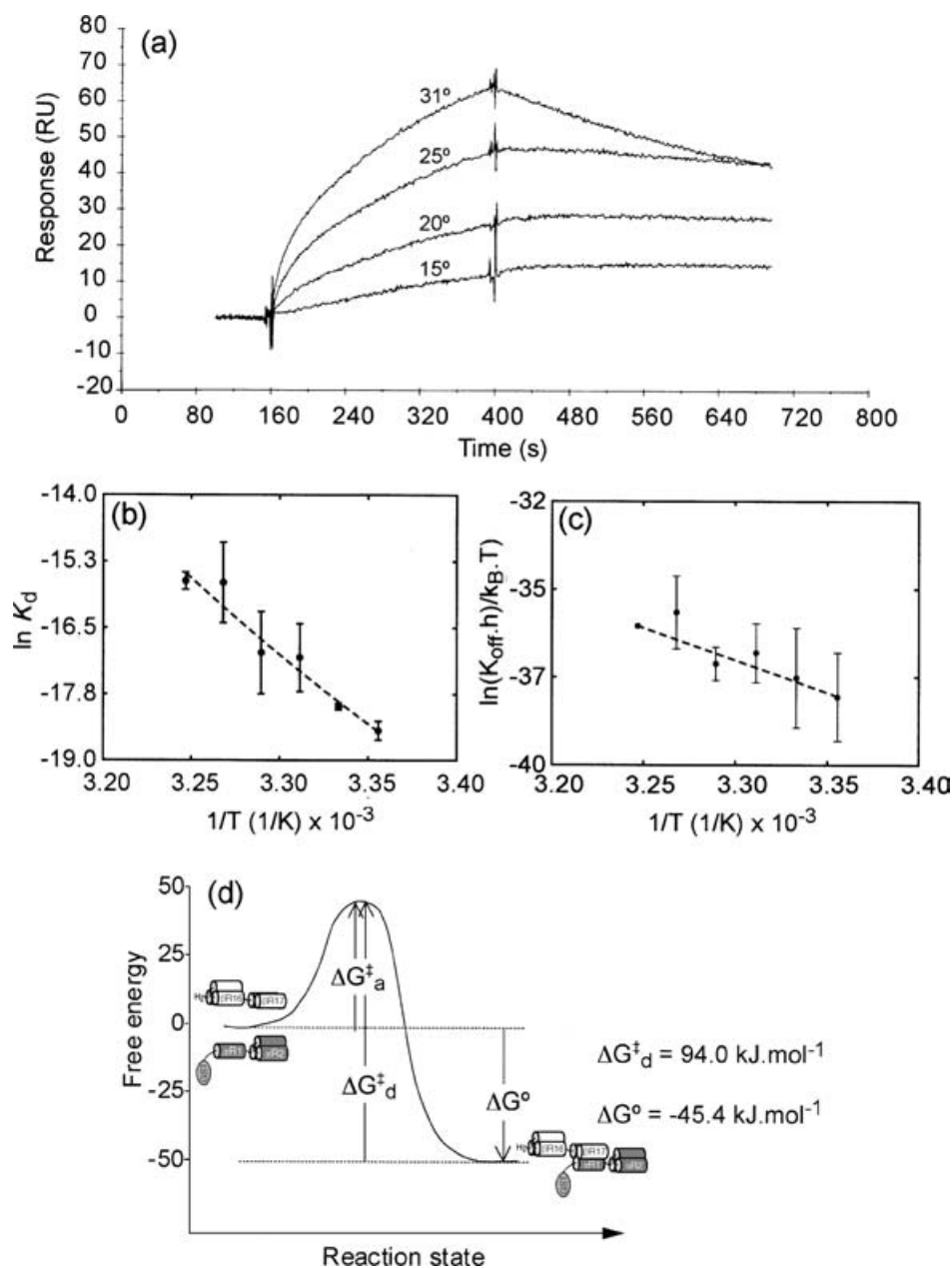


Figure 6 Thermodynamic analysis of α II- β II interaction

(a) Interaction was monitored by kinetic measurements injecting β II Σ 2 solutions of different concentrations at $20 \mu\text{l} \cdot \text{min}^{-1}$ over immobilized α II; binding data were collected with the BIAcore instrument equilibrated between 15 and 35 °C (sensorgrams are shown for the indicated temperatures only). Data collected at temperatures between 23 and 35 °C were used for the thermodynamic analysis. (b) van't Hoff plot for the interaction. The line was determined from linear least squares fitting of the van't Hoff equation. (c) Eyring plot for the dissociation phase of the reaction. (d) Free-energy profile for α II- β II Σ 2 interaction representing the Gibbs free-energy change between the individual recombinant proteins and the interacting proteins forming the complex that resembles the tetramerization site in native spectrin. ΔG_d^+ is the change in Gibbs free energy between the transition state and the complexed proteins, calculated from (c). ΔG_a^+ is the Gibbs free-energy change required for the formation of the transition state, calculated as $\Delta G_a^+ = \Delta G^{o\dagger} + \Delta G_d^+$.

damaging the fusion protein on the surface; >10–12 consecutive binding and regeneration cycles could be performed in each surface before it started losing some of the binding capacity (Figure 4). In all cases, high-quality data were obtained when the sensorgrams for each interaction were double referenced by subtraction of the sensorgram corresponding to the control GST flowcell and a blank run with buffer only.

The α constructs used in these assays retained their GST-fusion partners for capture on the BIAcore chip. In principle, GST could interfere with the assay. In practice, we believe this

not to be the case. As noted both in the Results section and below, we have confidence in the assay because the results for α I and β I constructs give affinities very similar to those found by others. Furthermore, in collaboration with the group of Dr Narla Mohandas (New York Blood Center, New York, NY, U.S.A.) we have used the α constructs as inhibitors of spectrin-tetramer formation in erythrocyte ghosts either with GST or after GST removal by thrombin (methods as in [27]). In this assay, the presence of the GST fusion makes no difference to the effectiveness of α construct interaction with membrane-bound β (X. An,

Table 3 Kinetic parameters for the interaction of α II- β II Σ 2 at different temperatures

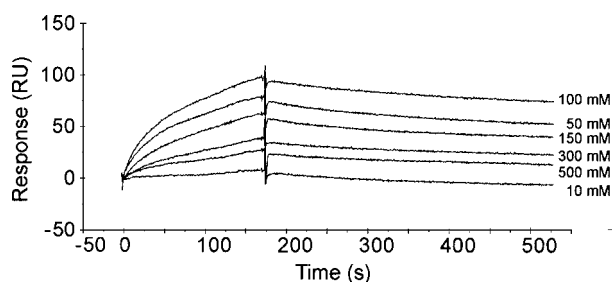
Rate constants for association (k_{on}) and dissociation (k_{off}) were calculated for β II Σ 2 (at concentrations of 0.2, 0.5, 1.0, 1.5 and 2.0 μ M) over captured GST- α II at 150 RU using kinetic measurements of the interactions at the specified temperature. The affinity of the interaction is shown as K_d .

Temperature ($^{\circ}$ C)	k_{on} ($M^{-1} \cdot s^{-1}$)	k_{off} (s^{-1})	K_d (nM)
35	11500	1.88×10^{-3}	163.5
33	11900	2.03×10^{-3}	170.6
31	22060	8.5×10^{-4}	38.5
29	32300	8.0×10^{-4}	24.8
27	24900	3.7×10^{-4}	14.9
25	24700	2.1×10^{-4}	8.5

Table 4 Thermodynamic parameters

Thermodynamic parameters of the equilibrium (a) and the transition state (b) for the interaction of α II- β II Σ 2.

(a)	
Parameter	Value
ΔG° ($kJ \cdot mol^{-1}$)	-45.5
ΔH° ($kJ \cdot mol^{-1}$)	-245
ΔS° ($kJ \cdot mol^{-1} \cdot K^{-1}$)	-0.67
(b)	
Parameter	Value
$\Delta G_{\ddagger}^{\ddagger}$ ($kJ \cdot mol^{-1}$)	94.0
$\Delta H_{\ddagger}^{\ddagger}$ ($kJ \cdot mol^{-1}$)	163.0
$\Delta S_{\ddagger}^{\ddagger}$ ($kJ \cdot mol^{-1} \cdot K^{-1}$)	0.23

**Figure 7 Salt sensitivity of α II- β II Σ 2 interaction**

Sensorgrams showing the binding of solutions of β II Σ 2 (1 μ M) to immobilized α II with the indicated NaCl concentration in the medium. Maximum binding is observed at physiological concentration of NaCl.

G. Debnath, W. Nunomura, A. Baines, W. Gratzner and N. Mohandas, unpublished work).

To validate the SPR assay, we used two approaches. The BIAcore analysis was compared with a 'pull-down' assay in which α II and β II Σ 2 polypeptides were allowed to associate in free solution, and then the complex was isolated (Figure 2). This yielded an estimate for the K_d of 29 nM, comparable with the value obtained from the BIAcore using both kinetic and equilibrium titration methods (approx. 9 nM; see Figures 4 and 5).

A second comparison comes from the well-characterized interaction of erythroid spectrin subunits: in the BIAcore kinetic

assay, K_d for this was measured as 840 ± 80 nM at 25 $^{\circ}$ C. Nicolas et al. [11] used similar constructs in an electrophoretic assay and obtained a K_d of approx. 900 ± 90 nM. In a microtiter plate competition assay, Cherry et al. [9] obtained an IC_{50} of approx. 800 nM at this temperature (inferred from Figure 5 in [9]). Other workers have not used directly comparable constructs for this measurement: for example, both Kennedy et al. [8] and DeSilva et al. [28] used an 80 kDa tryptic fragment of α I spectrin to bind to isolated β I subunits, and obtained K_d values of 2.2–2.3 μ M at 23 $^{\circ}$ C. It is difficult to compare these data directly with ours, given the differences in preparations and methods used, especially since the tryptic fragment lacks the six N-terminal amino acid residues of α I spectrin (compare the amino acid sequence of this fragment [29] with sequence deduced from the cDNA [30]). Nevertheless, the good agreement between the data of Nicolas et al. [11], Cherry et al. [9] and the data shown here gives confidence in the method. The rate constants for this reaction indicate that it is very low ($k_{on} = 59.4 M^{-1} \cdot s^{-1}$; $k_{off} = 5 \times 10^{-5} s^{-1}$). Neither of the studies using directly comparable constructs [9,11] obtained rate constants. DeSilva et al. [28] measured k_{on} for the 80 kDa α I tryptic fragment interacting with isolated β monomer and obtained a value of $144 M^{-1} \cdot s^{-1}$ at 23 $^{\circ}$ C. Our data indicate a lower k_{on} by a factor of just over 2. There are (to our knowledge) no direct measurements of k_{off} for α I and β I constructs equivalent to ours, but DeSilva et al. [28] inferred k_{off} from direct measurements of K_d and k_{on} ; they estimated a value of $3.4 \times 10^{-4} s^{-1}$ at 23 $^{\circ}$ C. Our measured k_{off} is an order of magnitude lower.

The high affinity of the α II- β II interaction is consistent with observations of the stability of purified brain spectrin tetramers after extraction at 37 $^{\circ}$ C [15]. α II binds both 'long' and 'short' C-terminal variants with very similar affinities (K_d of 67 ± 2 nM and 60 ± 8 nM respectively), although the rates of reaction are very different (e.g. the k_{on} values for α II interacting with β II Σ 1 and β II Σ 2 are $2.6 \times 10^5 M^{-1} \cdot s^{-1}$ and $2.5 \times 10^4 M^{-1} \cdot s^{-1}$ respectively). Mechanisms underlying the differences in rate constants can only be speculated on at this stage, but do not appear to derive from overall folding (since we determined that the constructs were correctly folded). The lack of effect of the C-terminal extensions on overall affinity is consistent with measurements of the interaction of α I with 'long' and 'short' C-terminal variants of β I spectrin (β I Σ 2 and β I Σ 1 respectively) and tail-less β I constructs [8,11,31]. The affinities are, however, much greater for α II- β II than for α I- β I ($K_d < 10$ nM and 842 nM respectively). The high affinity of this reaction is associated with a high enthalpy ($-245 kJ \cdot mol^{-1}$ in Figure 6 and Table 4). The enthalpy is greater than equivalent measurements on α I and β I fragments, which indicate -65 – $69 kJ \cdot mol^{-1}$ [28]. The activation energy for the forward reaction ($\alpha + \beta \rightarrow \alpha\beta$) we estimated at $48 kJ \cdot mol^{-1}$, very similar to erythroid spectrin fragments ($50 kJ \cdot mol^{-1}$ [28]). This high activation energy probably accounts for the very low association rate at low temperatures: in the BIAcore, it was impractical to measure the interaction at temperatures lower than 23 $^{\circ}$ C.

Early observations of spectrin purified from brain revealed that it had a much stiffer appearance than erythroid spectrin [15,32]. This appearance led to the suggestion that the apparent preferential formation of brain spectrin tetramers arises from inability to form closed-loop dimers. Our data suggest that high-affinity interaction of α II and β II chains can account for tetramer stability.

Figure 7 and the SPR assay regeneration scheme (Figure 3) show that the interaction is sensitive to ionic strength, and binding is most favoured at approx. 0.1 M NaCl. These data are strongly analogous to the behaviour of erythroid spectrin: Ungewickell and Gratzner [13], and Cole and Ralston [33] showed that the

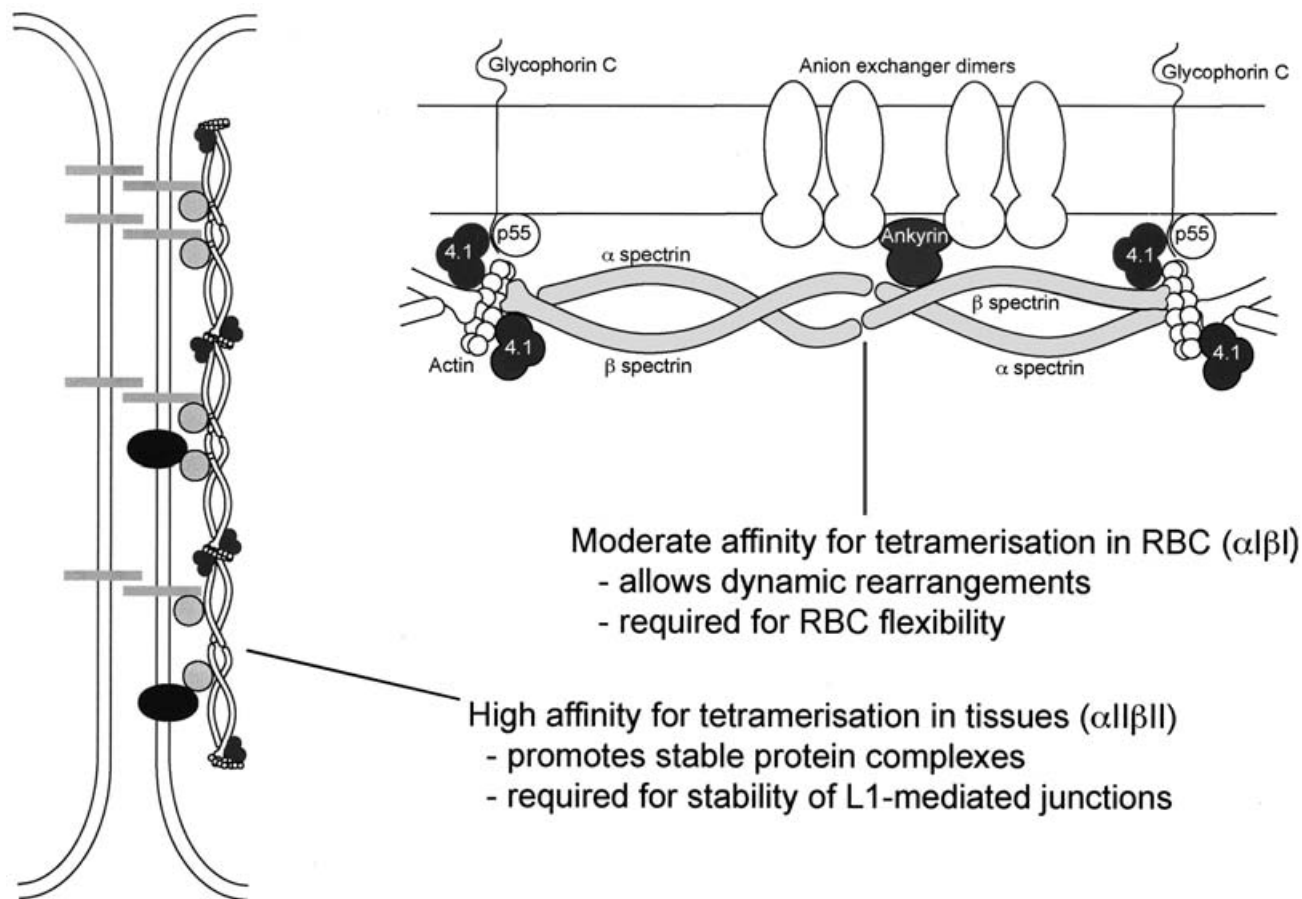


Figure 8 Possible significance of α - β spectrin affinities

Proposed meaning of the different affinity interactions observed for α I- β I complexes in erythrocytes and α II- β II complexes in solid tissues. RBC, red blood cell.

interaction of dimers to form tetramers is optimal at ionic strength of approx. 0.1 M at $<20^\circ\text{C}$ (although such an effect was not found by Cherry et al. [9] at 4°C). Both Bennett et al. [15] and Begg et al. [34] found that brain spectrin tetramers dissociate in >0.3 M NaCl. It seems probable that the major interactions of α II and β II are both ionic and hydrophobic (both urea and high salt are required to separate α II and β II). Begg et al. [34] examined the interactions of brain spectrin dimers in high-salt solutions: they suggested an affinity for brain spectrin tetramerization some 15-fold higher than that for erythroid spectrin, but since they used total brain spectrin (a complex mixture of isoforms) in non-physiological salt solutions, it is difficult to compare their results with ours. Recently, Park et al. [35] identified salt bridges between α and β subunits at the tetramerization site in a modelled structure of brain spectrin that are not present in the erythrocyte structure determined by NMR, which could account for the difference in their affinity. Park et al. [35] also suggested a role for the disordered conformation of the junction region (between the single helix C in α R1 and the α R2) during self-association.

One of the most striking aspects of our analysis is the result from the chimaeras. We exchanged the partial triple-helical repeats (α R1) between the α I and α II constructs, so that chimaeras containing α IR1 next to α IIR2, and α IIR1 next to α IR2, were formed. If the characteristics of binding depended only on α R1, then it should make no difference that R2 is next to R1. However, Table 2 indicates that α R2 has a major effect on binding affinity, and that the effect on affinity varies with β isoforms as described is

detailed in the Results section. The chimaeras reveal a previously unsuspected role for α R2, and possibly point to interactions of this repeat with the C-terminal extensions that characterize each isoform, such that the rates of reaction are affected. Previous observations (e.g. [11]) on erythroid spectrin have indicated a role for α R2 in stabilizing the structure of α R1. Two possibilities might account for the effect of α R2 on the affinity of interaction with β subunits: α IR2 and α IIR2 might have differential effects on α R1 structure; alternatively (or in addition), there might be an interaction of α R2 with β subunits. The latter possibility was not supported by a recent modelling study of the α I- β I spectrin interaction [36]; however, our own preliminary modelling of the α - β complex reveals a possible contribution of residues at the turn between B and C helices of α R2 (results not shown). It will be important to solve this by high-resolution structural analysis: initial crystallization attempts are in progress.

In tissues where α I, α II, β I and β II spectrins are all expressed within the same cell, it has been observed that tetramers tend to contain primarily α I- β I or α II- β II [37]. The rapid and high-affinity interaction of α II- β II is likely to contribute to the segregation of isoforms.

The functions of 'non-erythroid' spectrins, exemplified by α II and β II, have been described as 'integrating cells into tissues' [1]. In solid tissues, spectrins have a major role in stabilizing cell-cell and cell-matrix adhesions, and the tetramer is vital to this. Loss of either α or β spectrins in nematodes or *Drosophila* results in loss of cell-cell contact in tissues subject to mechanical stress

(reviewed in [1]). In erythrocytes, the comparatively moderate affinity of α I- β I tetramerization contributes to dynamic rearrangements of the cytoskeleton as membranes are subjected to the shearing forces of circulation [27]. Such dynamic rearrangements might not be desirable where strong cell adhesions are required, schematically represented in Figure 8. In epithelial cells, spectrin has been shown to exist predominantly in cytoplasmic or membrane-bound states, depending on the stage of the cell cycle [38] or on the formation of intercellular junctions [39]. High-affinity interaction of non-erythroid α and β spectrins is likely to ensure retention of tetrameric state even at low concentration in the cytoplasm. On the other hand, when tissue structures are modified during development, or in response to extracellular stimuli, it might be necessary to moderate the high affinity of the α II- β II interaction. Regulation of tissue spectrin tetramerization will be an important topic for future investigation.

We thank Dr Walter Gratzer for helpful comments on the manuscript. Helpful discussions with Dr Amarbalita Bhambra (BIA Applications Specialist, BIAcore AB) are acknowledged. This work was funded by project grants from the British Heart Foundation and the Biotechnology and Biological Sciences Research Council, and by a Network grant from the European Union. Equipment grants from the Wellcome Trust are acknowledged.

REFERENCES

- Bennett, V. and Baines, A. J. (2001) Spectrin and ankyrin-based pathways: metazoan inventions for integrating cells into tissues. *Physiol. Rev.* **81**, 1353–1392
- Tse, W. T. and Lux, S. E. (1999) Red blood cell membrane disorders. *Br. J. Haematol.* **104**, 2–13
- Deng, H., Lee, J. K., Goldstein, L. S. and Branton, D. (1995) *Drosophila* development requires spectrin network formation. *J. Cell Biol.* **128**, 71–79
- Djinovic-Carugo, K., Gautel, M., Ylanne, J. and Young, P. (2002) The spectrin repeat: a structural platform for cytoskeletal protein assemblies. *FEBS Lett.* **513**, 119–123
- Tse, W. T., Lecomte, M. C., Costa, F. F., Garbarz, M., Feo, C., Boivin, P., Dhermy, D. and Forget, B. G. (1990) Point mutation in the β -spectrin gene associated with α I/74 hereditary elliptocytosis: implications for the mechanism of spectrin dimer self-association. *J. Clin. Invest.* **86**, 909–916
- Kotula, L., DeSilva, T. M., Speicher, D. W. and Curtis, P. J. (1993) Functional characterization of recombinant human red cell α -spectrin polypeptides containing the tetramer binding site. *J. Biol. Chem.* **268**, 14788–14793
- Speicher, D. W., DeSilva, T. M., Speicher, K. D., Ursitti, J. A., Hembach, P. and Weglarz, L. (1993) Location of the human red cell spectrin tetramer binding site and detection of a related "closed" hairpin loop dimer using proteolytic footprinting. *J. Biol. Chem.* **268**, 4227–4235
- Kennedy, S. P., Weed, S. A., Forget, B. G. and Morrow, J. S. (1994) A partial structural repeat forms the heterodimer self-association site of all β -spectrins. *J. Biol. Chem.* **269**, 11400–11408
- Cherry, L., Menhart, N. and Fung, L. W. (1999) Interactions of the α -spectrin N-terminal region with β -spectrin: implications for the spectrin tetramerization reaction. *J. Biol. Chem.* **274**, 2077–2084
- Mehboob, S., Luo, B. H., Patel, B. M. and Fung, L. W. (2001) α β Spectrin coiled coil association at the tetramerization site. *Biochemistry* **40**, 12457–12464
- Nicolas, G., Pedroni, S., Fournier, C., Gautero, H., Craescu, C., Dhermy, D. and Lecomte, M. C. (1998) Spectrin self-association site: characterization and study of β -spectrin mutations associated with hereditary elliptocytosis. *Biochem. J.* **332**, 81–89
- Lecomte, M. C., Nicolas, G., Dhermy, D., Pinder, J. C. and Gratzer, W. B. (1999) Properties of normal and mutant polypeptide fragments from the dimer self-association sites of human red cell spectrin. *Eur. Biophys. J.* **28**, 208–215
- Ungewickell, E. and Gratzer, W. (1978) Self-association of human spectrin: a thermodynamic and kinetic study. *Eur. J. Biochem.* **88**, 379–385
- Morrow, J. S. and Marchesi, V. T. (1981) Self-assembly of spectrin oligomers *in vitro*: a basis for a dynamic cytoskeleton. *J. Cell Biol.* **88**, 463–468
- Bennett, V., Davis, J. and Fowler, W. E. (1982) Brain spectrin, a membrane-associated protein related in structure and function to erythrocyte spectrin. *Nature (London)* **299**, 126–131
- Glenney, Jr, J. R., Glenney, P. and Weber, K. (1982) F-actin-binding and cross-linking properties of porcine brain fodrin, a spectrin-related molecule. *J. Biol. Chem.* **257**, 9781–9787
- Shahbakhti, F. and Gratzer, W. B. (1986) Analysis of the self-association of human red cell spectrin. *Biochemistry* **25**, 5969–5975
- Davis, J. and Bennett, V. (1983) Brain spectrin: isolation of subunits and formation of hybrids with erythrocyte spectrin subunits. *J. Biol. Chem.* **258**, 7757–7766
- Hayes, N. V., Scott, C., Heerkens, E., Ohanian, V., Maggs, A. M., Pinder, J. C., Kordeli, E. and Baines, A. J. (2000) Identification of a novel C-terminal variant of β II spectrin: two isoforms of β II spectrin have distinct intracellular locations and activities. *J. Cell Sci.* **113**, 2023–2034
- Pace, C. N., Vajdos, F., Fee, L., Grimsley, G. and Gray, T. (1995) How to measure and predict the molar absorption-coefficient of a protein. *Protein Sci.* **4**, 2411–2423
- MacDonald, R. I., Musacchio, A., Holmgren, R. A. and Saraste, M. (1994) Invariant tryptophan at a shielded site promotes folding of the conformational unit of spectrin. *Proc. Natl. Acad. Sci. U.S.A.* **91**, 1299–1303
- Scott, C., Phillips, G. W. and Baines, A. J. (2001) Properties of the C-terminal domain of 4.1 proteins. *Eur. J. Biochem.* **268**, 3709–3717
- Laemmli, U. K. (1970) Cleavage of structural proteins during the assembly of the head of bacteriophage T4. *Nature (London)* **227**, 680–685
- Myszka, D. G. (2000) Kinetic, equilibrium, and thermodynamic analysis of macromolecular interactions with BIACORE. *Methods Enzymol.* **323**, 325–340
- Zeder-Lutz, G., Zuber, E., Witz, J. and Van Regenmortel, M. H. (1997) Thermodynamic analysis of antigen-antibody binding using biosensor measurements at different temperatures. *Anal. Biochem.* **246**, 123–132
- Yoshino, H. and Marchesi, V. T. (1984) Isolation of spectrin subunits and reassociation *in vitro*: analysis by fluorescence polarization. *J. Biol. Chem.* **259**, 4496–4500
- An, X., Lecomte, M. C., Chasis, J. A., Mohandas, N. and Gratzer, W. (2002) Shear-response of the spectrin dimer-tetramer equilibrium in the red blood cell membrane. *J. Biol. Chem.* **277**, 31796–31800
- DeSilva, T. M., Peng, K. C., Speicher, K. D. and Speicher, D. W. (1992) Analysis of human red cell spectrin tetramer (head-to-head) assembly using complementary univalent peptides. *Biochemistry* **31**, 10872–10878
- Speicher, D. W., Davis, G. and Marchesi, V. T. (1983) Structure of human erythrocyte spectrin: II. The sequence of the α -I domain. *J. Biol. Chem.* **258**, 14938–14947
- Sahr, K. E., Laurila, P., Kotula, L., Scarpa, A. L., Coupal, E., Leto, T. L., Linnenbach, A. J., Winkelmann, J. C., Speicher, D. W., Marchesi, V. T. et al. (1990) The complete cDNA and polypeptide sequences of human erythroid α -spectrin. *J. Biol. Chem.* **265**, 4434–4443
- Luo, B. H., Mehboob, S., Hurtuk, M. G., Pipalia, N. H. and Fung, L. W. (2002) Important region in the β -spectrin C-terminus for spectrin tetramer formation. *Eur. J. Haematol.* **68**, 73–79
- Glenney, Jr, J. R., Glenney, P. and Weber, K. (1982) Erythroid spectrin, brain fodrin, and intestinal brush border proteins (TW-260/240) are related molecules containing a common calmodulin-binding subunit bound to a variant cell type-specific subunit. *Proc. Natl. Acad. Sci. U.S.A.* **79**, 4002–4005
- Cole, N. and Ralston, G. B. (1992) The effects of ionic strength on the self-association of human spectrin. *Biochim. Biophys. Acta* **1121**, 23–30
- Begg, G. E., Morris, M. B. and Ralston, G. B. (1997) Comparison of the salt-dependent self-association of brain and erythroid spectrin. *Biochemistry* **36**, 6977–6985
- Park, S., Caffrey, M. S., Johnson, M. E. and Fung, L. W. (2003) Solution structural studies on human erythrocyte α -spectrin tetramerization site. *J. Biol. Chem.* **278**, 21837–21844
- Zhang, Z., Weed, S. A., Gallagher, P. G. and Morrow, J. S. (2001) Dynamic molecular modeling of pathogenic mutations in the spectrin self-association domain. *Blood* **98**, 1645–1653
- Clark, M. B., Ma, Y., Bloom, M. L., Barker, J. E., Zagon, I. S., Zimmer, W. E. and Goodman, S. R. (1994) Brain α erythroid spectrin: identification, compartmentalization, and β spectrin associations. *Brain Res.* **663**, 223–236
- Fowler, V. M. and Adam, E. J. (1992) Spectrin redistributes to the cytosol and is phosphorylated during mitosis in cultured cells. *J. Cell Biol.* **119**, 1559–1572
- Nelson, W. J. and Veshnock, P. J. (1987) Modulation of fodrin (membrane skeleton) stability by cell-cell contact in Madin-Darby canine kidney epithelial cells. *J. Cell Biol.* **104**, 1527–1537

Received 4 April 2003/23 June 2003; accepted 23 June 2003

Published as BJ Immediate Publication 23 June 2003, DOI 10.1042/BJ20030507